Resonant photoemission of anatase TiO_2 (101) and (001) single crystals

A. G. Thomas,* W. R. Flavell, A. R. Kumarasinghe, A. K. Mallick, D. Tsoutsou, and G. C. Smith
Physics Department, UMIST. P.O. Box 88 Manchester, M60 1QD, United Kingdom

R. Stockbauer
Department of Physics, Louisiana State University, Baton Rouge, Louisiana 70803

S. Patel
CLRC Daresbury Laboratory, Warrington WA5 4AD, United Kingdom

M. Grätzel and R. Hengerer
Swiss Federal Institute of Technology, Institute of Photonics and Interfaces, Chemin des Alambics, CH-1015 Lausanne, Switzerland
(Received 15 July 2002; published 16 January 2003)

The resonant behavior of anatase TiO_2 (101) and (001) surfaces has been investigated using synchrotron photoemission spectroscopy. The data are compared with earlier photoemission work from rutile TiO_2(110) and calculations for bulk anatase in order to elucidate the degree of Ti-O hybridization in the valence band. The results for the (101) surface show good general agreement with bulk band-structure calculations. Deviations from the bulk band structure in the case of the (001) surface are attributed to the reconstruction of this surface. A small peak is observed at around 1 eV binding energy (relative to the Fermi energy) for both surfaces following the creation of surface defects (O vacancies), which is thought to arise from surface Ti^{3+}. The attenuation of this peak by gentle heating in O_2 is attributed to healing of the surface O vacancies.

DOI: 10.1103/PhysRevB.67.035110 PACS number(s): 79.60.Bm, 79.60.Dp

I. INTRODUCTION

For some time there has been much interest in TiO_2 due to its applications in catalysis,[1] gas sensor devices,[2] and pigments and more recently its use in biomaterial coatings.[3] In addition, there has been recent interest in anatase phase TiO_2 nanocrystals produced by a sol-gel route for applications in photocatalysis[4,5] and solar cells,[6–8] to name but a few. The rutile form of TiO_2 has been widely studied[9–18] due to the ready availability of bulk single crystals, with the electronic structure having been widely investigated by x-ray photoemission spectroscopy[9] (XPS), ultraviolet photoemission spectroscopy[10] (UPS), and resonant photoemission spectroscopy.[11–14] The geometric structure of the most stable rutile surfaces [namely (100), (110), and (001)] have also been widely investigated by low-energy electron diffraction[15] (LEED), photoelectron diffraction,[16] scanning tunneling microscopy[17] (STM), and surface x-ray diffraction[18] (SXRD).

It appears from recent density-functional calculations that the surface energy of certain faces of the anatase crystal is lower than that of rutile, thus stabilizing the anatase form in the nanocrystals, as the surface/bulk ratio is large.[19] In addition, the anatase form also seems to exhibit more potent photocatalytic properties in its bulk form than rutile. Until 1999 only one photoemission study of the anatase surface existed in the literature;[20] however, the recent availability of good-quality grown anatase single crystals and thin films and the applications mentioned above is producing a renewed interest in this polymorph of TiO_2.

Resonant photoemission uses the fact that certain photoemission spectral features increase or decrease in amplitude as the photon energy is swept through the optical absorption edge of a constituent atom of the material.[11–14,21] The direct Ti $3p$ photoemission process is given by

$$3p^6 3d^n + h\nu \rightarrow 3p^6 3d^{n-1} + e^-. \quad (1)$$

However, at the $3p \rightarrow 3d$ optical absorption edge we see a resonance due to interference between the direct photoemission process and the excitation of electrons from the $3p$ to the $3d$ orbital followed by a super-Coster-Kronig decay into a continuum state. These two steps can be summarized as

$$3p^6 3d^n + h\nu \rightarrow [3p^5 3d^{n+1}]^* \rightarrow 3p^6 3d^{n-1} + e^-. \quad (2)$$

The asterisk denotes an excited state. This resonance process would only be expected to occur for features associated with the occupied metal-ion $3d$ orbitals but is known to occur for features associated with the O $2p$ valence band in transition-metal (TM) oxides, even those with d^0 configurations such as TiO_2, as a result of strong hybridization of the cations with their oxygen ligands.[11,12,21] The presence of a resonance in parts of the valence band then allows us to make some assumptions about the origin of features observed in the photoemission spectrum and the nature of the bonding associated with such features.

Here we measure and discuss high-resolution valence-band and resonance photoemission spectra of the *in vacuo* prepared TiO_2 anatase (101) and (001) surfaces. The data are discussed with reference to previous work for the rutile phase of TiO_2 and calculations of the bulk density of states (DOS) for anatase.

II. EXPERIMENT

TiO_2 anatase crystals [4 mm×2 mm (101) and 3×2 mm (001) (Ref. 22)] were grown by a chemical transport method.[23] The single crystals were characterized by Laue back reflection, which showed no evidence of twinning, LEED, and secondary-electron diffraction[22] prior to the photoemission measurements being made. The orientation of the surface under investigation was confirmed by simulations of the Laue pattern using Lauegen software.[24]

For these experiments the samples were mounted in a UHV chamber by means of Ta clips on a 316L stainless steel backplate. The base pressure in the chamber was around 5×10^{-10} Torr during the photoemission measurements. The chamber, equipped with an ARUPS10 multichannel hemispherical analyzer, electron gun, LEED, and Ar^+-ion etching, is described in detail elsewhere.[25] Sample preparation was performed by cycles of 500 eV Ar^+ sputtering for 10 min followed by 30 min of heating to 600 °C by e^- bombardment on the back of the sample plate. The sample temperature was measured using a thermocouple attached to the sample plate. Annealing was carefully controlled to limit surface reconstruction and to ensure no phase transitions occurred.[22] This treatment resulted in a sharp (1×1) LEED pattern for the (101) crystal and a (1×4) LEED pattern from the (001) surface in agreement with previous LEED measurements from these surfaces[22,26] and calculations of the surface energy.[19,27] The samples were determined to be free of contamination by electron Auger spectroscopy. Oxygen dosing was performed by admitting oxygen gas (MG Special gases 99.999%) via a high-precision leak valve with exposure in langmuirs ($1\ \mathrm{L}=1\times10^{-6}$ Torr s) monitored by an RGA placed in the main chamber. During oxygen exposure the sample was heated to around 400 K.

Photoemission measurements were recorded on the multipole wiggler beamline MPW6.1 (PHOENIX, photon energy range 30 eV$\leqslant h\nu\leqslant$350 eV) at the CLRC Daresbury Laboratory SRS.[28] Energy distribution curves (EDC's) were recorded with the sample at an angle of 45° to the incident photons and close to normal electron emission. Constant-initial-state (CIS) spectra were recorded in the same geometry with a fixed photon energy increment of 0.2 eV. All spectra were recorded with the sample at room temperature and, where appropriate, are referenced to a Fermi edge recorded from a sputtered Ta clip holding the sample in place and normalized to the *Io* (flux) monitor of the beam line. *Io* was recorded using a W mesh placed in the beam line just prior to the point where light enters the experimental chamber. The total resolution was 140 meV as determined from a Fermi edge spectrum recorded from the sputtered Ta clip.

III. RESULTS AND DISCUSSION

A. Resonance behavior of anatase TiO_2 (101) and (001) as prepared *in vacuo*

Figure 1 shows the valence-band EDC's recorded at photon energies of 40–80 eV from the (101) crystal. The spectra are in excellent agreement with previous EDC's recorded from natural anatase using an x-ray source.[20] The spectra

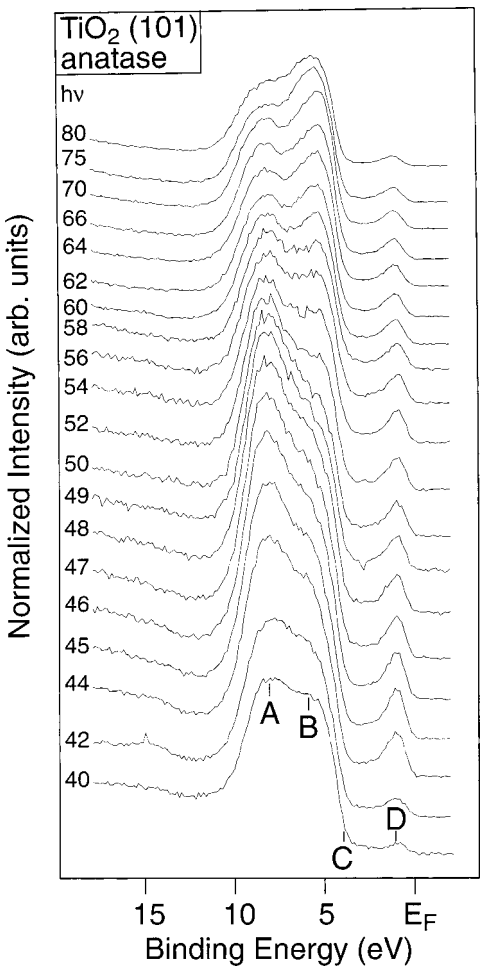

FIG. 1. EDC's of the clean TiO_2 anatase (101) surface at increasing photon energies. The points marked *A*, *B*, *C*, and *D* refer to the binding energies at which CIS spectra were recorded. *A* = 8.2 eV, *B* = 5.4 eV, *C* = 4.0 eV, *D* = 1.1 eV.

also show a resemblance to those recorded from the rutile form of TiO_2, in that there are two main peaks in the valence band at binding energies of 5.4 and 8.2 eV and a small defect peak at a binding energy of 1.1 eV.[10,12–14] The two peaks at 5.4 and 8.2 eV are expected to be derived mainly from O $2p$ states as in the case of rutile TiO_2.[12] It is clear from the spectra presented in Fig. 2 that the valence-band features undergo resonance between photon energies of around 42 and 60 eV, a region normally associated with the Ti $3p\rightarrow3d$ threshold.[11–14] Resonance of these features is attributed to strong Ti-O hybridization,[13,29–31] as one would not expect O states to resonate at these energies, i.e., the resonance occurs via the interatomic decay channel[11,21]

$$\mathrm{Ti}\ \ 3p^5 3d^1 + \mathrm{O}\ \ 2p^6 \rightarrow [\mathrm{Ti}\ \ 3p^6 3d^0]^* + \mathrm{O}\ \ 2p^6 \rightarrow \mathrm{Ti}\ \ 3p^6 3d^0 + \mathrm{O}\ \ 2p^5 + e^-. \quad (3)$$

The resonance of valence-band features marked *A* and *B* in Fig. 1 is shown more clearly in Fig. 2. In addition to the 47 eV resonance we see a broad shoulder for both features *A*

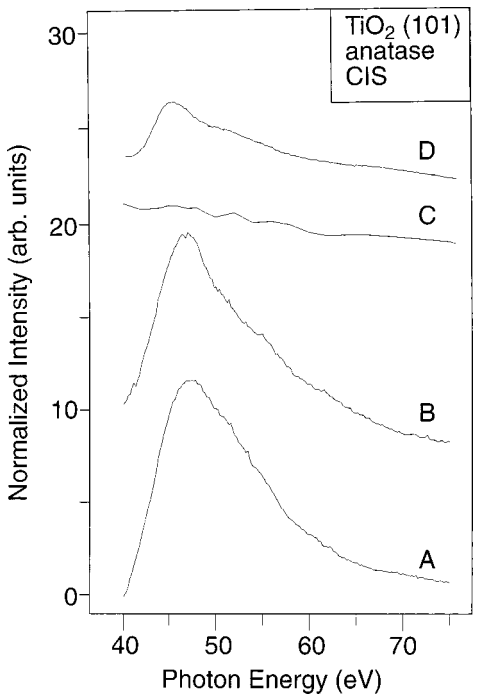

FIG. 2. CIS spectra of the features *A*, *B*, *C*, and *D* of the valence-band spectrum of anatase (101) labeled in Fig. 1. *A*, *B*, and *D* are recorded CIS spectra; *C* is reconstructed from the EDC's in Fig. 1. The spectra have been arbitrarily offset on the intensity scale for ease of viewing.

and *B* at around 55–60 eV. The energies of these two resonances are similar to those observed for rutile TiO_2(110),[12,13] where the feature at around 47 eV is assigned to an optical Ti $3p \rightarrow 3d$ excitation process and that at around 50–60 eV to Ti $3p \rightarrow 4s$ excitation.[12–14,32]

Recent calculations on bulk anatase allow a more detailed assignment of the features of the anatase valence band. The fully linearized augmented plane-wave (FLAPW) calculations of Asahi *et al.*[29] show Ti $3d$ states to be present throughout the valence band with the exception of the very lowest binding energy region of the valence band, which is attributed almost solely to O $2p_\pi$ states. The DOS calculations for bulk stoichiometric anatase TiO_2 of Asahi *et al.*[29] compared to a recorded EDC from the (101) TiO_2 anatase surface and the molecular orbital (MO) diagram derived from the DOS are presented in Fig. 3. A photon energy of 80 eV is used as it represents the energy at which the O $2p$ and Ti $3d$ cross sections are closest in value in this work $[\sigma(\mathrm{O}\ 2p):\sigma(\mathrm{Ti}\ 3d) \sim 4:3]$.[32,33] The calculated spectra are aligned to the experiment at the valence-band maximum (VBM) as this was the zero of energy used by the authors.[29] Both the energy relative to VBM and the absolute binding energy (BE) relative to E_F are shown. The apparent agreement between the energy position of the defect state and the mainly Ti $3d$ states at around 1 eV BE is to some extent fortuitous. The $3d$ states in the calculation should, in fact, lie above the Fermi level as the calculation is for the *stoichiometric* surface, which has unoccupied Ti $3d$ states. However this type of calculation tends to underestimate the magnitude of the band gap. In contrast, our experimental spectrum indicates the presence of surface O vacancies in the form of surface Ti^{3+}, i.e., in the experimental spectrum we have occupied Ti $3d$ states and we thus observe a defect state below E_F similar to that observed on rutile TiO_2 surfaces.[10,12–14]

The MO diagram shown in Fig. 3 indicates the highest binding-energy part of the valence band to be the most strongly hybridized resulting from overlap between O $2p_\sigma$ and Ti e_g states, with small contributions from Ti t_{2g} and $4s$. This is supported by the resonance profile in Fig. 2 recorded for feature *A*, where we see a strong resonance at around 47 eV from Ti $3p \rightarrow 3d$ optical transitions, with a broad shoulder at around 55–60 eV, which is attributed to Ti $3p \rightarrow 4s$ transitions as described for rutile.[12,14]

It is clear from Fig. 2 that for feature *B* (5.4 eV BE), although the general shape of the resonance is the same as that for feature *A*, the resonance is weaker overall than that from feature *A* (8.2 eV BE). The weaker resonance arises presumably as a result of the reduced hybridization of Ti with O in this region of the valence band, though the DOS calculations in Fig. 3 show that some Ti $3d$ character remains in this part of the valence band. The MO picture for anatase in Fig. 3(b) shows overlap of O $2p_\pi$ and Ti t_{2g} in this part of the valence band. The resonance at 47 eV agrees with this. However, we still see a broad, weak shoulder at around 50–60 eV, which is again presumably linked to $p \rightarrow s$ transitions. This may be due to reduced symmetry at the surface as the FLAPW calculations suggest there is no $4s$ character in the bulk anatase TiO_2 DOS (Ref. 29) in this part of the valence band. A reduction in symmetry at the surface is the reason given for the large resonance at around 55 eV in rutile TiO_2(110).[12,34] Unlike rutile, however, in the present work the 47 eV resonance is dominant throughout the valence band.

According to the calculated bulk DOS shown in Fig. 3(a) there appears to be very little contribution of the Ti $3d$ states at the very-lowest-energy part of the valence band, suggesting that there is little or no hybridization of Ti and O states at these energies. The CIS spectrum recorded at this energy (curve *C* in Fig. 2) shows no resonances at either 47 or 55 eV, apparently confirming the absence of Ti $3d$ states in this part of the valence band.

Feature *D*, the band-gap state, at 1.1 eV is clearly seen to undergo a resonance with the shoulder at 50–60 eV apparently much more pronounced. A similar effect was also seen for the defect state (or O-vacancy state) in rutile.[13] The resonance observed here suggests a contribution from Ti $3d$ to this state in anatase presumably as a result of surface O vacancies resulting in Ti^{3+}. Such vacancies have indeed been imaged on anatase surfaces by STM.[34,35] The observed increase in the Ti $3p \rightarrow 4s$ resonance intensity is somewhat at odds with the MO structure, which suggests no contribution from the Ti $4s$ states. This may be a consequence of the reduced symmetry at the surface or the reduced oxidation state of the Ti^{3+} ions. In addition to the difference in the shape of the profile it is also apparent that the peak position of the resonance for the defect peak has shifted down in energy to 45 eV at the peak intensity maximum (the shoulder is also shifted down to around 52 eV as compared to 55 eV for the features *A* and *B*, though the absence of a clear peak

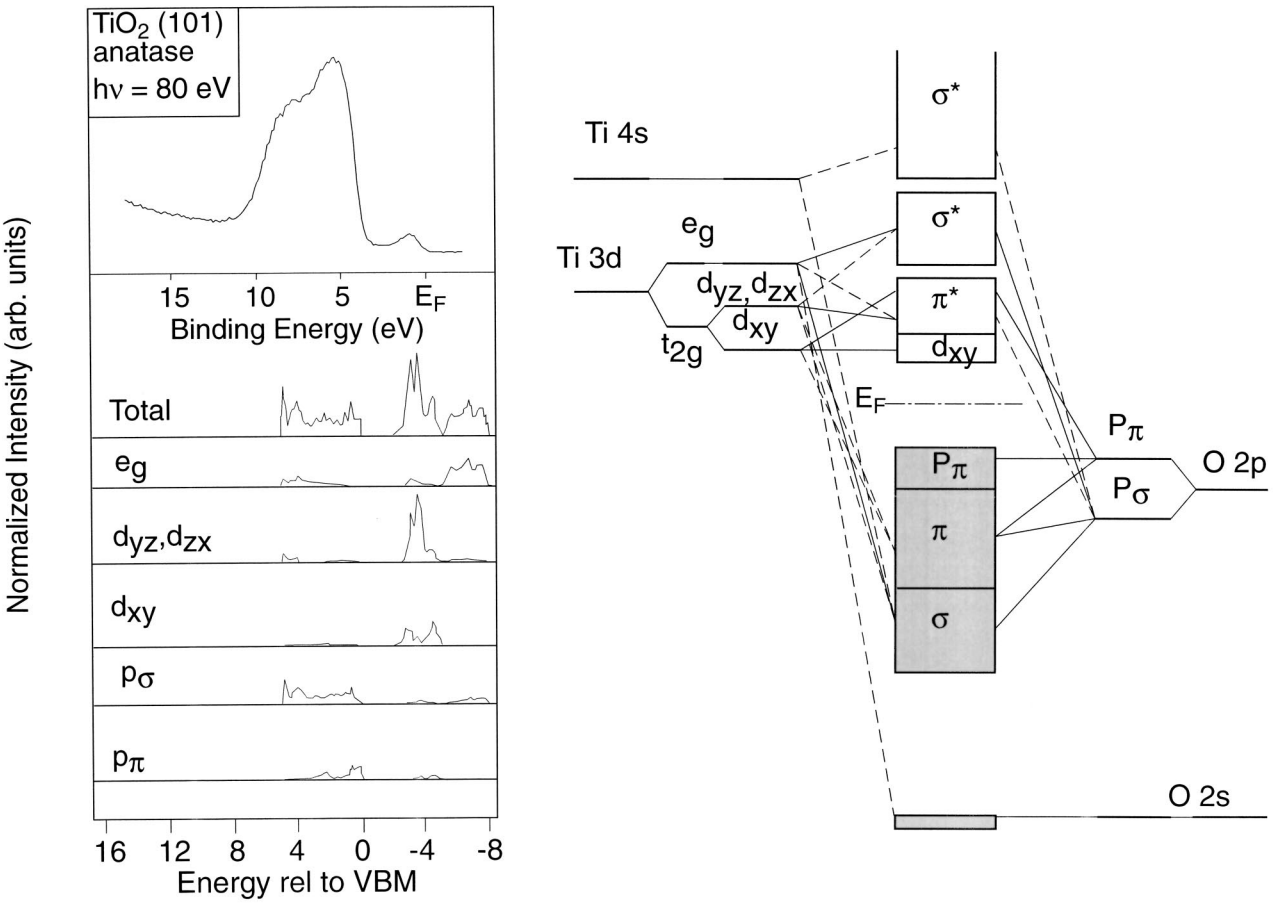

FIG. 3. (a) Comparison of the experimental EDC of anatase TiO_2(101) recorded at 80 eV photon energy with the bulk band-structure calculations of Asahi *et al.* (Ref. 29). The calculations have been aligned with experiment at the valence-band maximum (see text). (b) MO diagram adapted from Ref. 29 showing the contributions to different parts of the valence band from the atomic states of Ti and O.

makes this energy more difficult to pinpoint precisely). This downward shift in energy is also consistent with the defect peak arising from reduced valency Ti^{3+} states at the surface and has been observed in other mixed-valency oxide systems.[36]

Figure 4 shows the valence-band EDC spectra of the (001) surface of anatase recorded at photon energies of 40–80 eV. Generally the spectra are similar to those recorded from the (101) surface. It is clear that the valence-band features undergo a resonance process between 40 and 60 eV. The most obvious difference lies in the intensity of the defect state, associated with the presence of Ti^{3+} at the surface. This feature is so weak that it can only just be resolved at around the maximum resonance energies (46–48 eV), indicating that the (1×4) surface reconstruction shows little or no Ti^{3+} at the surface. The absence of Ti^{3+} at the surface is in agreement with Ti $2p$ XPS from the (1×4) reconstructed (001) surface.[26,37] This seems to suggest that the (001) (1×4) surface is more stable with respect to reduction than the (101) surface, and the low index surfaces of rutile TiO_2. Indeed, as will be discussed in Sec. III B below, 1.5 keV Ar^+ sputtering followed by annealing was required to produce the defect state at the (001) surface.

The CIS spectra in Fig. 5, for the features marked *A* and *B* in Fig. 3, are broadly similar to those recorded from the (101) surface. There are, however, some subtle differences. First for feature *A*, there appears to be no contribution to the spectrum at 55 eV associated with the Ti $3p\rightarrow4s$ resonance. The resonance profiles recorded from the (001) surface for both features *A* and *B* are narrower than their analogs on the (101) surface, although feature *B* exhibits a weak shoulder at around 55 eV, suggesting $4s$ character. The peak resonance of feature *A* occurs at 47 eV compared to 48 eV for feature *B* and the two resonances appear to be of similar intensity. It therefore appears that the (1×4) reconstruction leads to a complete restructuring of the DOS on this surface with a modification of the Ti-O hybridization over all parts of the valence band. Further evidence for this change in bonding character in the valence band comes from the CIS spectrum recorded at 4 eV binding energy (feature *C*).

For the (001) surface we see two very clear peaks at photon energies of 46.5 and 53–54 eV, in marked contrast to the (101) surface. From the discussion above the higher-energy feature is associated with Ti $3p\rightarrow4s$ resonance. However, the FLAPW calculations for anatase,[29] shown in Fig. 3, and rutile[31] suggest there should be no Ti $4s$–derived states in this part of the valence band, and indeed none is observed for the (101) surface (Fig. 2). This result then suggests that the

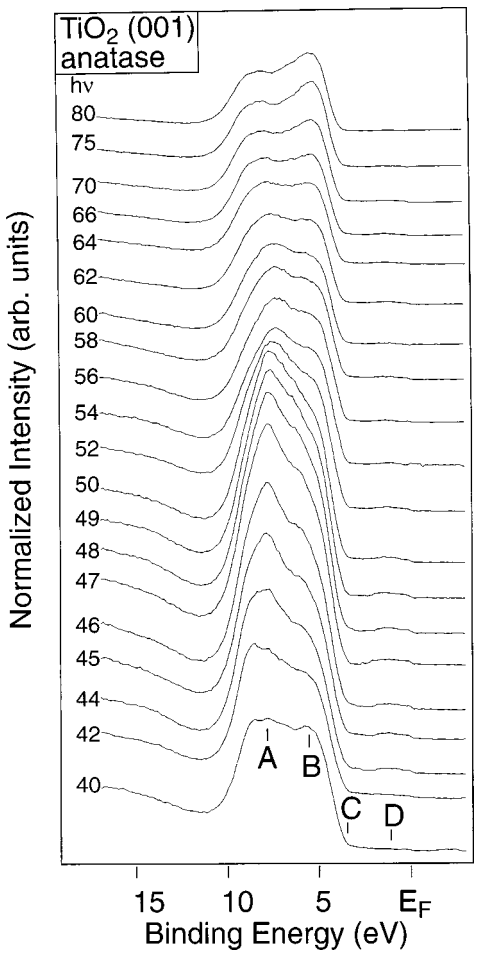

FIG. 4. EDC's from the clean TiO_2 anatase (001) surface at increasing photon energies. The points marked *A*, *B*, *C*, and *D* refer to the binding energies at which CIS spectra were recorded. $A = 8.2$ eV, $B = 5.4$ eV, $C = 4.0$ eV, $D = 1.1$ eV.

significant geometrical structure rearrangement at the (001) surface has a great effect on the bonding and therefore the electronic structure. This is not surprising since it has been shown that the (1×4) surface reconstruction ''admolecule model'' of Lazzeri and Selloni[27] has average Ti-O bond lengths of 1.84 Å compared to the (101) surface where, assuming a bulk termination, the average Ti-O distance is 1.93 Å.[20] A contraction of the fivefold Ti-O bond lengths would be expected to lead to an enhancement of Ti $4s-$O $2p^2$ overlap[14] and thus an increase in the amount of *s* character is sensible. One unexpected feature of the result is that the 4*s* contribution is localized so close to the valence-band maximum. The dramatic difference in the electronic structure between the (101) and (001) surfaces also almost certainly rules out any reconstructions based on a {101} microfacet model such as that proposed recently by Tanner, Young, and Altman.[38] Further elucidation of the structure would be enhanced by *surface* DOS calculations that would allow comparison with our experimental observations of the *surface* electronic structure of different anatase surfaces.

For completeness we add that for this surface, no resonance is observed for the defect state in the CIS. However, there is evidence of a resonance in the EDC spectra (Fig. 4) where a small bump may be observed at around 1 eV BE when the photon energy is around 47 eV. The weak resonance is attributed to the fact that there are in fact very few Ti^{3+} states on this surface as seen in Fig. 4. This result is in agreement with earlier work.[26,37] It is possible to create Ti^{3+} states on this surface by more extensive Ar^+-ion etching as described in Sec III B below.

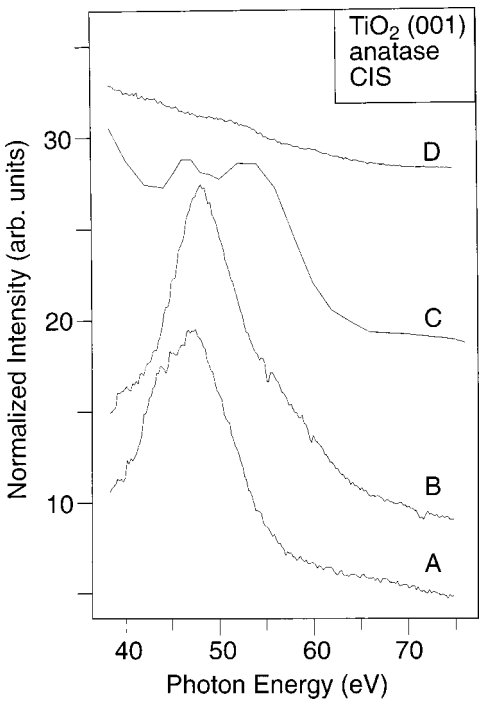

FIG. 5. CIS spectra of the features *A*, *B*, *C*, and *D* of the valence-band spectrum of anatase (001) labeled in Fig. 4. *A*, *B*, and *D* are recorded CIS spectra; *C* is reconstructed from the EDC's in Fig. 4. The spectra have been arbitrarily offset on the intensity scale for ease of viewing.

B. Behavior of the "defect peak" on oxygen adsorption

Figure 6 shows the effect of increasing oxygen exposure on the valence band and defect state of anatase (101) recorded at a photon energy of 48 eV. The clean TiO_2 anatase surface was prepared as described above before being gently heated and exposed to increasing oxygen coverages. The sample was allowed to cool to room temperature before each spectrum was recorded. It is clear that following O_2 exposure the defect state decreases in intensity as the exposure is increased, though it is still evident even following a 10^4 L exposure. On the rutile $TiO_2(110)$ surface 1 L O_2 exposure is sufficient to reduce the defect state intensity by half, though 10^8 L is required to remove it completely.[39] In addition to the effects on the defect peak we also see the appearance of a shoulder at BE of 9 eV on the valence band at the highest O_2 exposure (10^4 L). The origin of this peak is not clear though it may be associated with the development of the stoichiometric (101) anatase surface as indicated by recent calculations.[40]

The effect of oxygen exposure on the valence band and defect state of the (001) surface is shown in Fig. 7. The

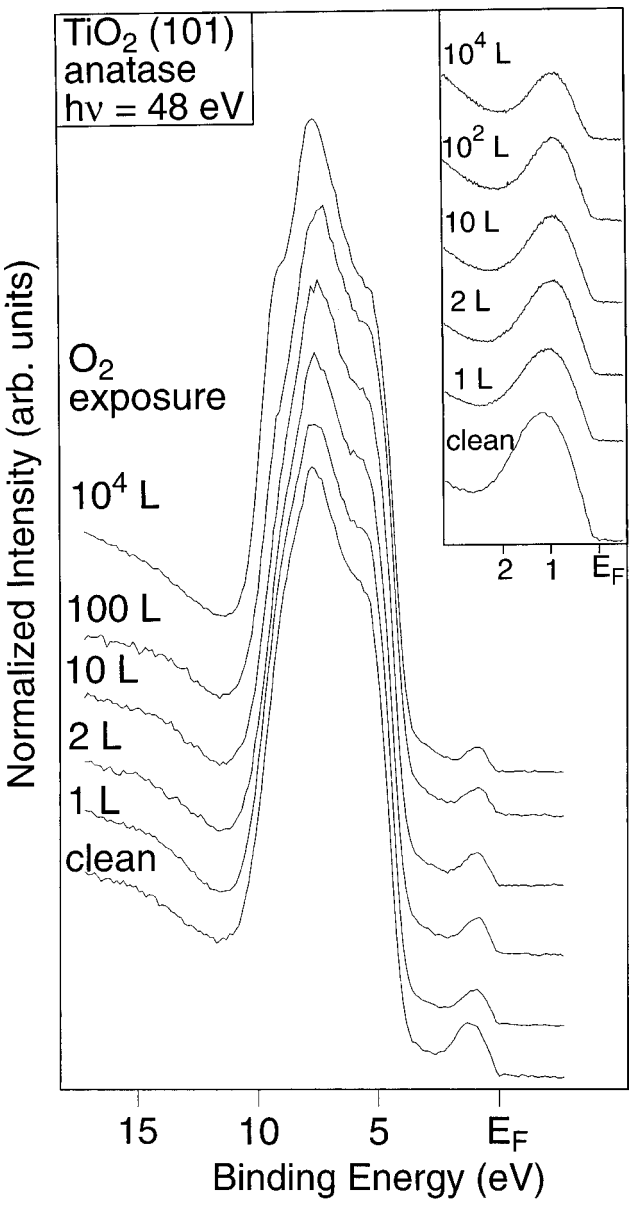

FIG. 6. Effect of oxygen adsorption the clean TiO_2 anatase (101) surface. The method of preparation is described earlier in the text. The inset shows the effect of O_2 adsorption on the defect state.

spectra are recorded at a photon energy of 48 eV. To introduce the defect state on the (001) surface required two cycles of 1.5 kV Ar^+ sputtering [cf. 500 eV required to prepare the (101) surface with defects] followed by annealing to 900 K. The stability of the (1×4) reconstructed anatase surface is well known.[26,37,38] Exposure to O_2 during gentle heating of the sample again leads to a gradual decrease in the intensity of the defect state. For both the (001) and (101) surfaces it is clear that the defect state is associated with O vacancies, which may be ''healed'' by exposure to O_2 under gentle heating conditions. This along with the resonance of the defect state suggests that it is due to the presence of Ti^{3+} resulting from surface O vacancies and in this respect the behavior of both surfaces is very similar to that observed for rutile.

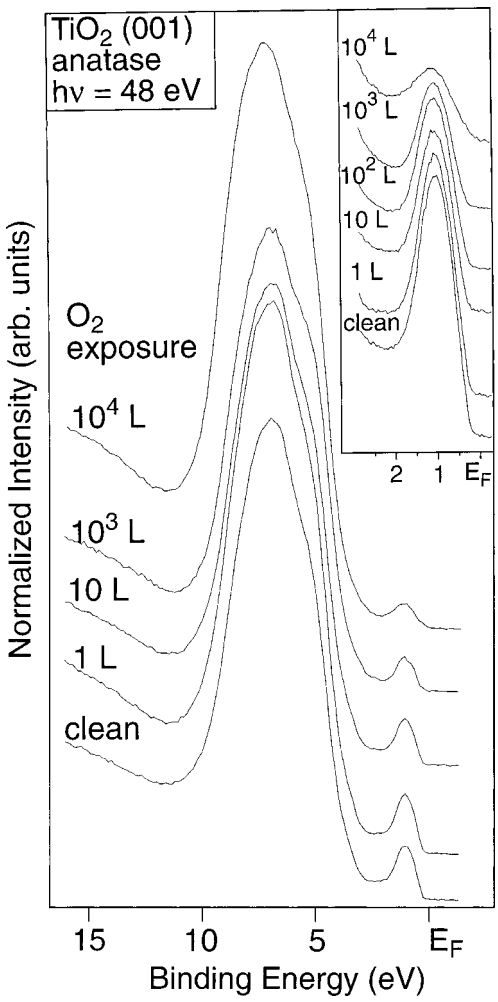

FIG. 7. Effect of oxygen adsorption on the TiO_2 anatase (001) surface following the creation of surface defects by two Ar^+ sputter/anneal cycles. The inset shows the effect of O_2 adsorption on the defect state.

IV. CONCLUSIONS

Resonant photoemission from the anatase (101) surface suggests the mainly O $2p$ valence band of anatase TiO_2 exhibits strong hybridization with Ti $3d$ and at the higher-binding-energy part of the valence band, Ti $4s$ states. At the lowest-energy part of the valence band there appears to be very little if any Ti contribution. These findings are in excellent agreement with FLAPW calculations for bulk anatase TiO_2. The band-gap state is also seen to undergo a resonance, and this in conjunction with the decrease in defect state intensity upon O adsorption leads us to conclude that the band-gap state is of Ti^{3+} character by analogy with the behavior of this feature in rutile.

The (001) surface is more complex. First, it undergoes a (1×4) reconstruction, which seems to stabilize the surface with regard to defect creation. We suggest that the reduction in bond length in conjunction with the overall geometrical rearrangement[19,27] leads to extensive changes in the hybridization between O $2p$ and Ti $3d/4s$ states compared both to the bulk DOS and the (101) surface DOS. Creation of O

vacancies may only be achieved by extensive Ar^+-ion bombardment. As for the (101) surface, this is thought to lead to Ti^{3+} at the surface, which may be reoxidized by exposure to molecular oxygen. For a thorough understanding of the hybridization, and the structure of the (001) surface in particular, detailed surface DOS calculations are required for comparison with the valence-band photoemission spectra.

ACKNOWLEDGMENTS

This work was funded by EPSRC. D.T. is funded by EPSRC, CLRC Daresbury Laboratory, and UMIST, G.C.S. is funded by EPSRC, and Johnson Matthey and A.K.M. are funded by BAEC and UMIST. We thank Michele Lazzeri and Anabella Selloni for helpful discussions. Thanks are also due Nigel Poolton and Frances Quinn at the SRS, CLRC Daresbury Laboratory.

*Corresponding author. Email address: a.g.thomas@umist.ac.uk

[1] A. Fujishima and K. Honda, Nature (London) **238**, 37 (1972).
[2] See, e.g., D. E. Williams in *Solid State Gas Sensing*, edited by P. T. Moseley and B. C. Tofield (Adam Hilger, Bristol, 1987).
[3] F. H. Jones, Surf. Sci. Rep. **42**, 75 (2001).
[4] A. Molinari, R. Amadelli, L. Antolini, P. Battioni, and D. Mansuy, J. Mol. Catal. A: Chem. **158**, 521 (2000).
[5] O. V. Makarova, T. Rajh, M. Thurnauer, A. Martin, P. A. Kemme, and D. Cropek, Environ. Sci. Technol. **34**, 4797 (2000).
[6] C. Barbe, F. Arendie, P. Comte, M. Jirosek, F. Lenmann, V. Shklover, and M. Grätzel, J. Am. Chem. Soc. **80**, 3157 (1997).
[7] K. Tennakone, A. R. Kumarasinghe, G. R. R. A. Kumara, K. Wijayantha, and P. M. Sirimanne, J. Photochem. Photobiol., A **108**, 193 (1997).
[8] A. R. Kumarasinghe and W. R. Flavell, J. Photochem. Photobiol., A **148**, 145 (2002).
[9] W. Göpel, J. A. Anderson, D. Frankel, M. Jähnig, K. Phillips, J. Schafer, and G. Rocker, Surf. Sci. **139**, 333 (1984).
[10] N. B. Brooks, D. S-L Law, T. S. Padmore, D. R. Warburton, and G. Thornton, Solid State Commun. **57**, 473 (1986).
[11] E. Bertel, R. Stockbauer, and T. E. Madey, Phys. Rev. B **27**, 1939 (1986); Surf. Sci. **141**, 355 (1984).
[12] Z. Zhang, S-P. Jeng, and V. E. Henrich, Phys. Rev. B **43**, 12004 (1991).
[13] R. Heise, R. Courths, and S. Witzel, Solid State Commun. **84**, 599 (1992).
[14] J. Nerlov, Q. Ge, and P. J. Møller, Surf. Sci. **348**, 28 (1996).
[15] P. W. Murray, F. M. Leibsle, C. A. Muryn, H. J. Fisher, C. F. J. Flipse, and G. Thornton, Surf. Sci. **321**, 217 (1994).
[16] P. J. Hardman, P. L. Wincott, G. Thornton, A. P. Kaduwela, and C. S. Fadley, Phys. Rev. B **60**, 11 700 (1999).
[17] H. Raza, C. L. Pang, S. A. Haycock, and G. Thornton, Phys. Rev. Lett. **82**, 5265 (1999).
[18] G. Charlton, P. B. Howe, C. L. Nicklin, P. Steadman, J. S. G. Taylor, C. A. Muryn, S. P. Harte, J. Mercer, R. McGrath, D. Norman, T. S. Turner, and G. Thornton, Phys. Rev. Lett. **78**, 495 (1997).
[19] M. Lazzeri, A. Vittadani, and A. Selloni, Phys. Rev. B **63**, 155409 (2001).
[20] R. Sanjines, H. Tang, H. Berger, F. Gozzo, G. Margaritondo, and F. Levy, J. Appl. Phys. **75**, 2945 (1994).
[21] L. C. Davies, J. Appl. Phys. **59**, R25 (1986).
[22] R. Hengerer, B. Bolliger, E. Erbudak, and M. Grätzel, Surf. Sci. **460**, 162 (2000).
[23] L. Kavan, M. Grätzel, S. E. Gilbert, C. Klemenz, and H. J. Scheel, J. Am. Chem. Soc. **118**, 6716 (1996).
[24] See, e.g., J. W. Campbell, J. Appl. Crystallogr. **28**, 228 (1995).
[25] P. G. D. Marr, Ph.D. thesis, UMIST, Manchester, UK (2001).
[26] Y. Liang, S. Gan, S. A. Chambers, and E. I. Altman, Phys. Rev. B **63**, 235402 (2001).
[27] M. Lazzeri and A. Selloni, Phys. Rev. Lett. **87**, 266105 (2001).
[28] M. Bowler, J. B. West, F. M. Quinn, D. M. P. Holland, B. Fell, P. A. Hatherly, I. Humphrey, W. R. Flavell, and B. Hamilton, Surf. Rev. Lett. **9**, 577 (2002).
[29] R. Asahi, Y. Taga, W. Mannstadt, and A. J. Freeman, Phys. Rev. B **61**, 7459 (2000).
[30] A. Stashans, S. Lunell, and R. W. Grimes, J. Phys. Chem. Solids **57**, 1293 (1996).
[31] P. I. Sorantin and K. Schwarz, Inorg. Chem. **31**, 567 (1992).
[32] We note that in the work of Heise, Courths, and Witzel (Ref. 13) the presented resonance spectra are in fact an integrated resonance of the whole valence band, whereas in this work and that of Zhang, Jeng, and Henrich (Ref. 12) the photon-energy-dependent plots are considered separately for the individual features of the valence band.
[33] J. J. Yeh and I. Lindau, At. Data Nucl. Data Tables **32**, 1 (1985).
[34] W. Hebenstreit, N. Ruzycki, R. Herman, Y. Gao, and U. Diebold, Phys. Rev. B **62**, R16334 (2000).
[35] A. R. Kumarasinghe (unpublished data).
[36] E.g., W. R. Flavell, J. Hollingworth, J. F. Howlett, A. G. Thomas, Md. M. Sarker, S. Squire, Z. Hashim, M. Mian, P. L. Wincott, D. Teehan, S. Downes, and F. ER. Hancock, J. Synchrotron Radiat. **2**, 264 (1995).
[37] G. S. Herman, M. R. Sievers, and Y. Gao, Phys. Rev. Lett. **84**, 3354 (2000).
[38] R. E. Tanner, Y. Liang, and E. I. Altman, Surf. Sci. **506**, 251 (2002).
[39] V. E. Henrich, G. Dresselhaus, and H. J. Zeiger, J. Vac. Sci. Technol. **15**, 534 (1978).
[40] A. Selloni and M. Lazzeri (unpublished).